

# 3-D DMO operators in transversely isotropic media

Tariq Alkhalifah

*Phd Candidate, Center for Wave Phenomena  
Colorado School of Mines*

## ABSTRACT

The 3-D dip-moveout (DMO) operator in homogeneous transversely isotropic media with vertical symmetry axis (VTI media), unlike that in homogeneous isotropic media, has an out-of-plane (crossline) component. In general, this additional component has a shape that is opposite to that of the crossline component of the isotropic  $v(z)$  saddle shaped operator. The width of the crossline component of the VTI operator, in general, is overall smaller than that associated with isotropic  $v(z)$  media. When both typical anisotropy and inhomogeneity are combined, the net result is an operator with a smaller crossline component and a shape that is more influenced by the  $v(z)$  behavior. The large cost of a 3-D DMO operator, as well as the generally small crossline components associated with the DMO operator in VTI media, suggests the possibility, as is usually done for isotropic  $v(z)$  media, of just ignoring the contribution of the out-of-plane portion of the operator.

**Key words:** transverse isotropy, dip moveout, 3D

## Introduction

The dip-moveout (DMO) operator (impulse response) for isotropic homogeneous media in the common-offset domain is two-dimensional, with the shape of an ellipse. The parameters of this ellipse are controlled by the source-receiver offset,  $X$ , and the normal moveout (NMO) corrected time,  $t_n$ . In 3-D homogeneous isotropic media, the DMO operator remains an ellipse in the vertical plane that contains the sources and receivers (Figure 1a). On the other hand, as Meinnardus and Schleicher (1993), Dietrich and Cohen (1992), and Artley et al. (1993) have shown, that the DMO operator in vertically inhomogeneous [ $v(z)$ ] isotropic media is the familiar saddle shape surface (Figure 1b).

In the inline plane (i.e., the vertical plane containing the source and receiver locations), the isotropic  $v(z)$  operator can be well approximated by a squeezed version of the isotropic homogeneous ellipse (Hale and Artley, 1993). This approximation, however, ignores the crossline component of the  $v(z)$  operator. In fact, the crossline component of the DMO operator is often ignored in practice in favor of efficiency and accuracy. It is believed that, in many cases, the  $v(z)$  influence on the operator

is counteracted by the presence of anisotropy (Gonzalez et al., 1992), so that better focusing is obtained by using the simple homogeneous operator rather than a  $v(z)$  one. Alkhalifah (1996), however, showed that the influence of anisotropy on the inline component can exceed the influence of  $v(z)$ , requiring, in many cases, a more advance treatment, namely use of an anisotropic  $v(z)$  operator.

Although Figure 1b shows the full shape of the 3-D DMO operator, the perspective plot does not reveal the details needed for comparisons of the kinematics of DMO responses. Such details can be better seen by displaying the inline and crossline components of the operator, separately. Thus, for example, Figures 2 and 3 show inline and crossline cross-sections (through the apex) of the DMO responses shown in Figure 1 for isotropic homogeneous and  $v(z)$  media, respectively. This format will be used for most of the comparisons discussed in this paper. All operators shown correspond to an offset,  $X=1.5$  km/s, and a  $t_n=1.75$  s. Variation in these parameters mainly influences the size of the operator, which is predictable but is beyond the scope of this note. For the homogeneous medium, the background velocity equals 2.0 km/s, whereas for the  $v(z)$  media, velocity increases lin-

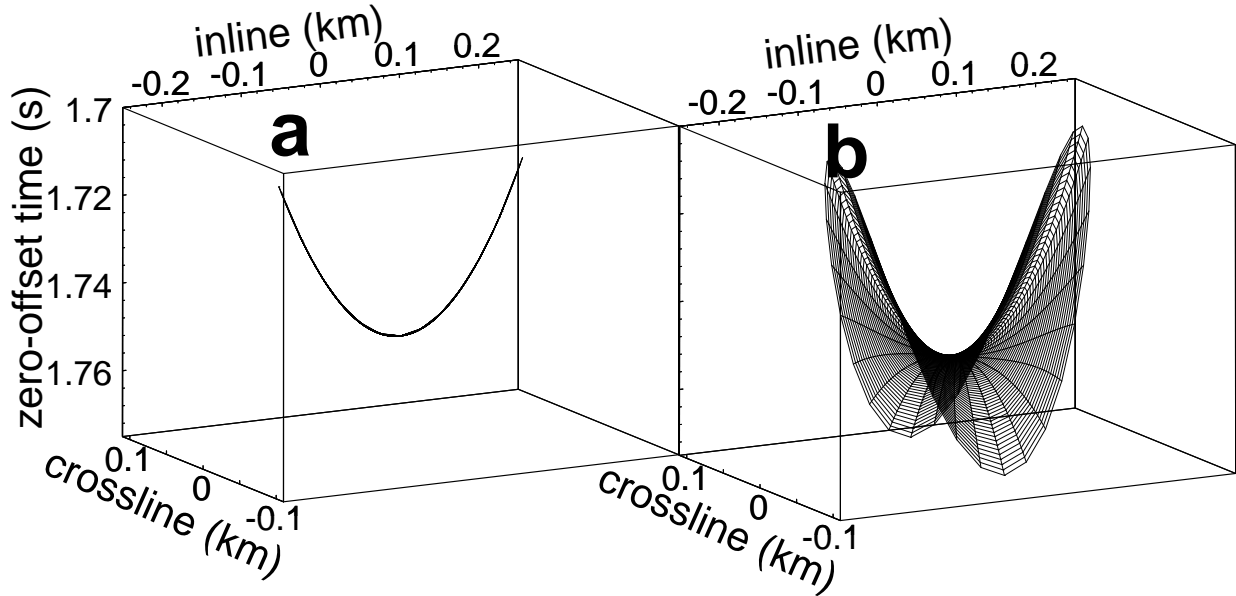


**Figure 1.** 3-D DMO operators for (a) a homogeneous isotropic medium with velocity equal 2.0 km/s, and (b) a vertically inhomogeneous isotropic medium with a surface velocity of 1.5 km/s and constant velocity gradient of 0.6 s<sup>-1</sup>. The root-mean-square velocity at the NMO-corrected time of 1.75 s is the same (2 km/s) for both models. The operator corresponds to a source-receiver offset of 1.5 km, which will be used throughout this paper.

early with depth with a constant velocity gradient,  $k=0.6$  s<sup>-1</sup> and an initial velocity at the surface,  $v_0=1.5$  km/s. Both velocity models result in the same root-mean-square (rms) velocity of 2 km/s at  $t_0 = 1.75$  s.

The crossline component of the isotropic homogeneous DMO operator, in Figure 2, is given by a single dot that represents the intersection of the crossline plane with the 2-D inline ellipse at its apex. The inline and crossline components of the  $v(z)$  isotropic operator in Figure 3 are largely as expected for the saddle shape shown in Figure 1b. The arrows in Figures 2 and 3 point to the reflector dip treated by this portion of the operator. Beyond a dip of about 75 degrees, the inline component shows a duplication that could not be clearly depicted in Figure 1b and was therefore not included in it.

Alkhalifah and Tsvankin (1995) demonstrated that, for TI media with vertical symmetry axis (VTI media), just two parameters are sufficient for performing all time-related processing, such as normal moveout (NMO) correction (including non-hyperbolic moveout correction, if necessary), dip-moveout (DMO) correction, and prestack and poststack time migration. One of these two parameters, the short-spread NMO velocity for a horizontal reflector, is given by

$$V_{\text{nmo}}(0) = V_{P0} \sqrt{1 + 2\delta}. \quad (1)$$

Taking  $V_h$  to be the  $P$ -wave velocity in the horizontal direction, the other parameter,  $\eta$ , is given by

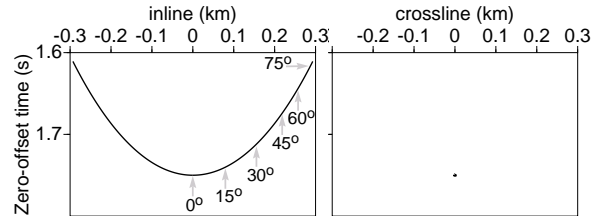


**Figure 2.** Inline and crossline sections through a 3-D DMO operator in a homogeneous isotropic medium for the same parameters used to generate Figure 1a.

$$\eta \equiv 0.5 \left( \frac{V_h^2}{V_{\text{nmo}}^2(0)} - 1 \right) = \frac{\epsilon - \delta}{1 + 2\delta}, \quad (2)$$

where  $V_{P0}$  is the  $P$ -wave vertical velocity, and  $\epsilon$  and  $\delta$  are Thomsen's (1986) dimensionless anisotropy parameters. Moreover, Alkhalifah and Tsvankin (1995) show that these two parameters,  $\eta$  and  $V_{\text{nmo}}$ , are obtainable solely from surface seismic  $P$ -wave data, specifically from estimates of stacking velocity for reflections from interfaces having two distinct dips (the DMO method). The two-parameter representation and inversion also holds in  $v(z)$  media. For DMO applications in two dimensions, Alkhalifah (1996) showed that  $\eta$  is the parameter responsible for the shape of the operator, whereas  $V_{\text{nmo}}(0)$  controls mainly the size of the operator, and a positive velocity gradient has the tendency to squeeze the operator.

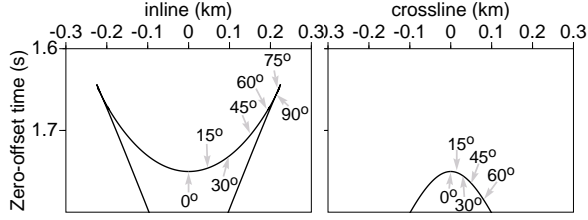


**Figure 3.** Inline and crossline components of a 3-D DMO operator in a  $v(z)$  isotropic medium for the same parameters used to generate Figure 1a. The arrows, here and thereafter, point to the portion of the operator that treats the indicated reflector dip.

In this paper, which is limited to just the kinematics, I show exact 3-D DMO operators for homogeneous and  $v(z)$  VTI media and give explanation for their unusual shapes. I also examine the influence of anisotropy on the DMO operator and compare it with the influence of vertical inhomogeneity. Finally, I draw conclusions regarding the importance of the out-of-plane component of the anisotropic 3-D DMO operator in practice.

### Generating the 3-D DMO Operator

Following Artley et al. (1993), I construct the 3-D DMO operator by solving a system of six nonlinear equations to obtain six unknowns that include, among other things, the zero-offset time and surface position of the specular reflection point. Artley's traveltimes are calculated and tabulated using an isotropic  $v(z)$  ray tracing. To construct the 3-D DMO operator for VTI media, modifications to Artley's method include honoring Snell's law for anisotropic media (recognizing the dependence of phase velocity on direction) as well as using anisotropic ray tracing to calculate traveltimes (Alkhalifah, 1996).

In either isotropic or anisotropic media, the zero-offset slowness vector  $\mathbf{p}_0$  is a scaled sum of the slownesses of the rays from the source  $\mathbf{p}_s$  and receiver  $\mathbf{p}_g$  to the specular point reflection. Thus,

$$\mathbf{p}_0 = \lambda(\mathbf{p}_s + \mathbf{p}_g). \quad (3)$$

Considering the z-component gives

$$p_{0z} = \lambda(p_{sz} + p_{gz}),$$

then

$$\lambda = \frac{p_{0z}}{p_{sz} + p_{gz}}.$$

Since

$$p_{0z} = \cos[\theta(p_0, t_0)]s(p_0, t_0),$$

$$p_{sz} = \cos[\theta(p_s, t_s)]s(p_s, t_s),$$

and

$$p_{gz} = \cos[\theta(p_g, t_g)]s(p_g, t_g),$$

where  $s$  is the slowness and  $\theta$  is the phase angle, both of which are calculated using ray tracing and tabulated as a function of rayparameter  $p$  and the traveltime  $t$ . Then

$$\lambda = \frac{\cos[\theta(p_0, t_0)]s(p_0, t_0)}{\cos[\theta(p_s, t_s)]s(p_s, t_s) + \cos[\theta(p_g, t_g)]s(p_g, t_g)}. \quad (4)$$

Substituting equation (4) into the  $x$ - and  $y$ -components of equation (3) provides two of the six nonlinear equations needed to be solved.

The other four equations are given by

$$0 = \xi(p_g, t_g) \cos \phi_g - \xi(p_s, t_s) \cos \phi_s + 2h \quad (5)$$

$$0 = \xi(p_g, t_g) \sin \phi_g - \xi(p_s, t_s) \sin \phi_s \quad (6)$$

$$0 = \tau(p_0, t_0) - \tau(p_s, t_s) \quad (7)$$

$$0 = \tau(p_0, t_0) - \tau(p_g, t_g), \quad (8)$$

Equation (5) is the requirement that the surface distances,  $\xi$ , along the inline component from each of the source and receiver to the specular reflection point (SRP) add up to equal the source-receiver offset,  $2h$ , and equation (6) is the requirement that the distances along the crossline component to SRP are equal for each of the source and receiver. Equations (7) and (8) imply that the vertical times,  $\tau$  (or depths) from each of the source, receiver, and zero-offset surface positions to SRP are the same. Like the slowness and phase angle,  $\xi$  and  $\tau$  are calculated using ray tracing and then stored in a table as a function of ray parameter  $p$  and the traveltime  $t$ .

This system of equations, like its 2-D counterpart (Artley and Hale, 1994; Alkhalifah, 1996) can be solved using Newton-Raphson iterative method (e.g., Press et al., 1986).

### 3-D DMO Operators in VTI Media

Figure 4 shows the inline and crossline components of the 3-D DMO operator in a homogeneous VTI medium, with  $V_{nmo}=2.0$  km/s and  $\eta=0.1$ . The inline component is the same as the 2-D operator shown by Alkhalifah (1996). Unlike the isotropic DMO operator, the anisotropic one has an out-of-plane component in a homogeneous medium. This out-of-plane component, moreover, is very different from that associated with isotropic  $v(z)$  media. The anisotropic operator is smaller in size than the  $v(z)$  one, and it is initially concaved upward. Based on the dip distribution along this operator, a reflection from an interface that is dipping at 75 degrees or more in crossline direction will be subjected to a simple time shift (almost no lateral migration). This time shift is needed to compensate for the difference between  $V_{nmo}(0)$ , the velocity

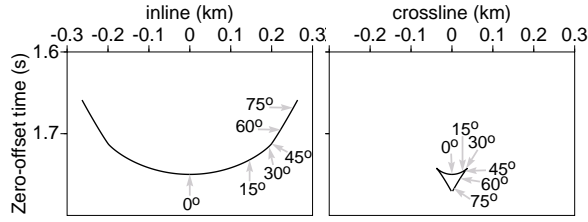


**Figure 4.** Inset and crossline components of a 3-D DMO operator in a homogeneous VTI medium with velocity equal 2.0 km/s and  $\eta = 0.1$ . As in Figure 1a, the offset,  $X = 1.5$  km and the NMO-corrected time,  $t_n = 1.75$  s.

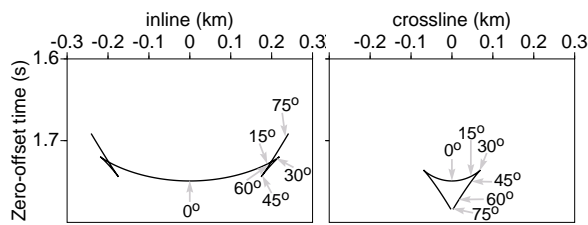


**Figure 5.** Inset and crossline components of a 3-D DMO operator in a homogeneous VTI medium with velocity equal 2.0 km/s and  $\eta = 0.2$ .

used in the NMO correction, and  $V_h$ , the actual normal moveout velocity for such a dip. This somewhat explains the presence of the duplication in the crossline component.

The inset and crossline components of the DMO operator for a stronger anisotropy ( $\eta=0.2$ ) are shown in Figure 5. The DMO operator is, in general, similar to that in Figure 4, with the features somewhat exaggerated; the inset component is further stretched with respect to the ellipse shape and exhibits triplication (Alkhalifah, 1996), and crossline component is larger with an even greater time shift for the reflector dip of 75 degrees (and larger) due to the larger difference between  $V_h$  and  $V_{nmo}(0)$ .

The combined influence of anisotropy and inhomogeneity on the DMO operator is shown in Figure 6. The medium is characterized by  $\eta = 0.1$ , and  $V_{nmo} = 1.5 + 0.6z$  km/s. Again, the inset component is the same as Alkhalifah (1996) and described in detail there. The crossline component has an overall concave downward shape with a small concave upward region caused by the anisotropy. Nevertheless, the domination of  $v(z)$  on the operator is apparent and, as a result, the general shape is largely a distorted saddle. Although, Alkhalifah (1996) demonstrated that, for a medium with the same inhomogeneity and anisotropy, the inset component (the 2-D operator) is dominated more by the anisotropy than by the vertical inhomogeneity (which results in an overall

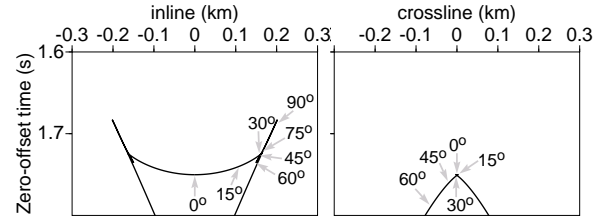


**Figure 6.** Inset and crossline components of a 3-D DMO operator in a  $v(z)$  VTI medium with velocity given by  $v(z) = 1.5 + 0.6z$  km/s and  $\eta = 0.1$ .

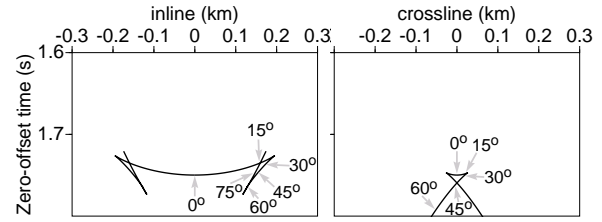


**Figure 7.** Inset and crossline components of a 3-D DMO operator in a  $v(z)$  VTI medium with velocity given by  $v(z) = 1.5 + 0.6z$  km/s and  $\eta = 0.2$ .

stretched operator rather than a squeezed one), the crossline component is dominated more by the inhomogeneity.

Note that the crossline component in Figure 6 is smaller than that in Figure 3, which implies that the anisotropy reduced the influence of  $v(z)$  on the operator. In fact, the crossline component is interesting because, up to 30-degree reflector dip, the crossline component is practically a point, similar to that for the homogeneous isotropic operator. The influences of inhomogeneity and anisotropy do not fully cancel, as Gonzalez et al. (1992) suggested, but less harm will be introduced in the data when this crossline component is ignored than when it is ignored for isotropic  $v(z)$  media.

A stronger anisotropy, given by  $\eta=0.2$ , gives a clearer picture of the triplication shown in Figure 6 (see Figure 7). Again the crossline component is smaller in size than the crossline component for purely isotropic  $v(z)$  media.

## Cost Issues

The computation cost for 3-D DMO operators is of an order magnitude higher than that for 2-D ones. Thus, for a simple Kirchhoff-type of DMO implementation (Deregowski, 1987), the cost of the 3-D DMO operator is about the cost of the 2-D operator multiplied by the

number of grid points needed to represent the crossline component of the 3-D DMO operator. In many cases, this additional cost may be considered to be unacceptable. Specifically, applying such a 3-D DMO followed by a post-stack time migration is comparable to the cost of a full 3-D prestack time migration.

Where seismic data are acquired along dip lines, 3-D DMO is not required, and therefore 2-D operators are dominant in practice. If ignoring the out-plane-component is acceptable in  $v(z)$  isotropic media, it should be more so in both homogeneous and  $v(z)$  VTI media because, in VTI media, the operator generally has a smaller crossline component than does that for typical isotropic  $v(z)$  media.

On the other hand, if the dominant reflector-dip direction was not taken into consideration during acquisition, dips with large crossline components will require use of a 3-D operator, whether the medium is isotropic or anisotropic.

## Discussion and Conclusions

The 3-D DMO operator in homogeneous VTI media, unlike that in homogeneous isotropic media, has an out-of-plane (crossline) component. In general, this additional component has a shape that is opposite to that of the crossline component of the isotropic  $v(z)$  saddle shaped operator. The crossline component of the VTI ( $\eta=0.1$ ) operator, as well as the inline component, are initially concaved upward (Figure 8a). The influence of a stronger anisotropy ( $\eta=0.2$ ) increases the breadth of the operator (Figure 9a). Nevertheless, the width of the crossline component of the VTI operator, in general, is overall smaller than that associated with isotropic  $v(z)$  media. When both typical anisotropy and inhomogeneity are combined, the net result is an operator with a smaller crossline component and a shape that is more influenced by the  $v(z)$  behavior (a saddle shape, see Figure 8b). In this case, the crossline component becomes less significant, with dips up to 30 degrees requiring practically no adjustment. Nevertheless, the inline component is controlled more by the anisotropy, causing the operator to stretch, rather than squeeze, relative to the elliptical operator for isotropic homogeneous media.

The large cost of a 3-D DMO operator, as well as the generally small crossline components associated with the DMO operator in VTI media, suggests the possibility, as is usually done for isotropic  $v(z)$  media, of just ignoring the contribution of the out-of-plane portion of the operator. Although on occasion it might be necessary to use a 3-D DMO operator, relying on a 2-D operator

is an attractive option that preserves the efficiency of a poststack migration processing sequence.

## Acknowledgments

I thank Ken Lerner for helpful discussions at the critical stages of this study and his review of the manuscript. This research is partially supported by the Advanced Computational Technology Initiative (ACTI), subcontract number B316649, in conjunction with Lawrence Livermore National Laboratory and industry project partners. It is also partially supported by the Center for Wave Phenomena Consortium Project at the Colorado School of Mines. I also wish to acknowledge the financial support from KACST (Saudi Arabia).

## REFERENCES

- Alkhalifah, T., 1996, Transformation to zero offset in transversely isotropic media: Geophysics, expected in the July-August issue.
- Alkhalifah, T., and Tsvankin, I., 1995, Velocity analysis for transversely isotropic media: Geophysics, **60**, 1550-1566.
- Artley C., Blondel P., Popovici A. M., and Schwab M., 1993, Three-dimensional dip moveout for depth-variable velocity: Colorado School of Mines; Center for Wave Phenomena report **CWP-137**.
- Artley, C., and Hale, D., 1994, Dip moveout processing for depth-variable velocity: Geophysics, **59**, 610-622.
- Deregowski, S. M., 1987, Integral implementation of dip moveout: Geophysical Transactions, **33**, 11-22.
- Dietrich, M., and Cohen, J. K., 1992, 3-D migration to zero offset for a constant velocity gradient: an analytical formulation: *submitted for publication in* Geophysical Prospecting; also published as Center for Wave Phenomena report **CWP-113**.
- Gonzalez, A., Levin, F. K., Chambers, R. E., and Mobley, E., 1992, Method of correcting 3-D DMO for the effects of wave propagation in an inhomogeneous earth, 62nd Ann. Internat. Mtg., Soc. Expl. Geophys., Expanded Abstracts, 966-969.
- Hale, D., and Artley, C. T., 1993, Squeezing DMO for depth-variable velocity: Geophysics, **58**, 257-264.
- Jakubowicz, H., 1990, A simple efficient method of dip-moveout correction: Geophys. Prosp., **38**, 221-245.
- Meinardus, H., and Schleicher, K., 1993, 3-D time-variant dip moveout by f-k method: Geophysics, **58**, 1030-1041.
- Press, W. H., Flannery, B. P., Teukolsky, S. A., and Vetterling, W. T., 1986, Numerical recipes: Cambridge Univ. Press.
- Thomsen, L., 1986, Weak elastic anisotropy: Geophysics, **51**, 1954-1966.

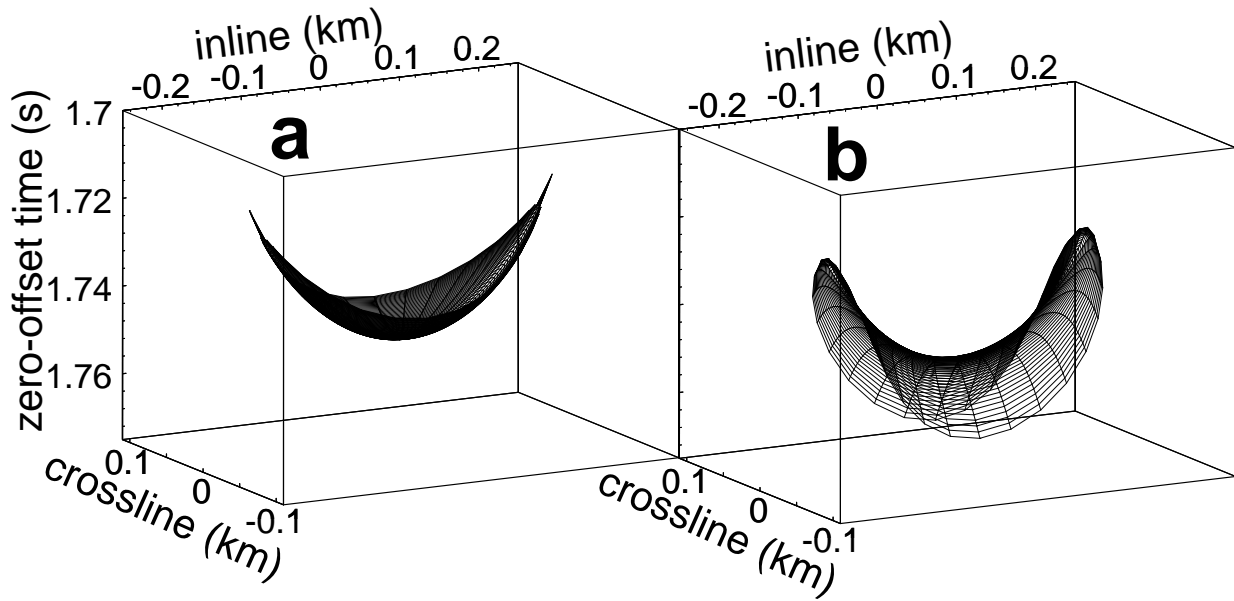


**Figure 8.** 3-D DMO operators for (a) a homogeneous VTI medium with velocity equal 2.0 km/s, and (b) a vertically inhomogeneous VTI medium with velocity given by  $v(z)=1.5+0.6z$  km/s. For both models,  $\eta=0.1$ . The operator, again, corresponds to an offset of 1.5 km.

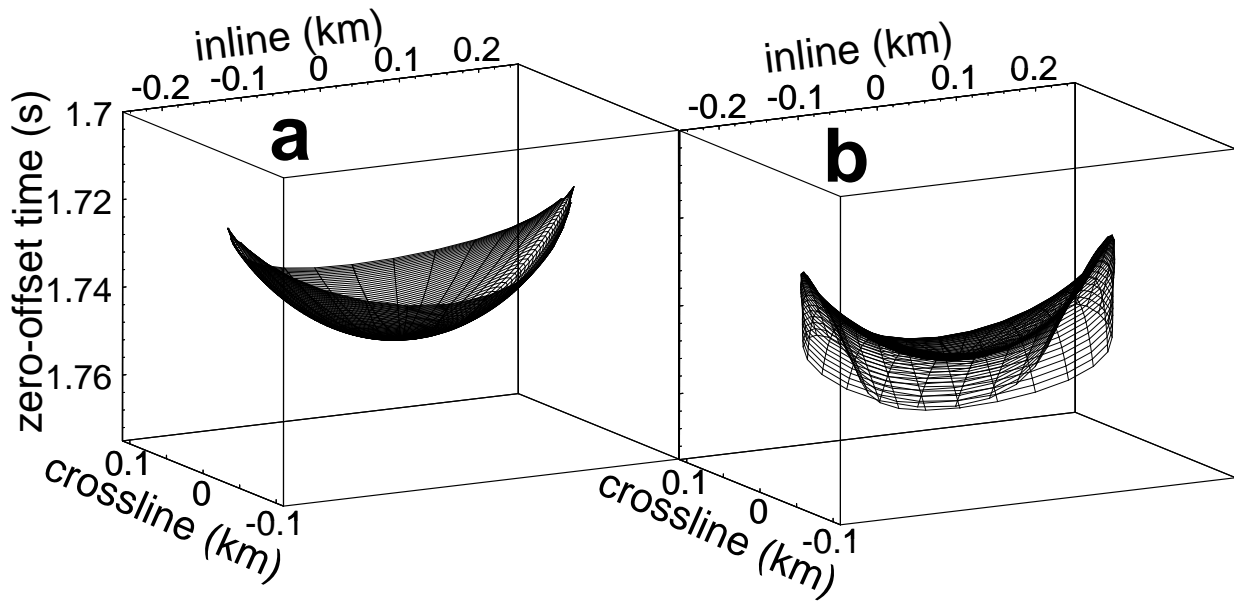


**Figure 9.** 3-D DMO operators for (a) a homogeneous VTI medium with velocity equal 2.0 km/s, and (b) a vertically inhomogeneous VTI medium with velocity given by  $v(z)=1.5+0.6z$  km/s. For both models,  $\eta$  now equals 0.2.